Effect of Higher-Order Silane Deposition on Spatial Profile of Si-H_2/Si-H Bond Density Ratio of a-Si:H Films*)

Liu SHI, Kazuma TANAKA, Hisayuki HARA, Shota NAGAISHI, Daisuke YAMASHITA, Kunihiro KAMATAKI, Naho ITAGAKI, Kazunori KOGA and Masaharu SHIRATANI

Kyushu University, Fukuoka 819-0395, Japan

(Received 7 January 2019 / Accepted 13 May 2019)

We studied how the deposition of SiH_3 radicals, higher-order silane molecules, and clusters contributed to the bond configuration of hydrogenated amorphous silicon (a-Si:H) films. In our experiment, the deposition of three species was controlled using a multi-hollow discharge plasma chemical vapor deposition (MHDPCVD) method using a cluster-eliminating filter. We reduced the incorporation of higher-order silane (HOS) molecules into the films by increasing the gas flow velocity in the hollows from 1008 to 2646 cm/s. The results show that the lower incorporation of HOS molecules into the films reduced the SiH_2/SiH bond ratio, i.e., I_{SiH2}/I_{SiH}. Moreover, two-dimensional profiles of the I_{SiH2}/I_{SiH} ratio and the surface morphology suggest that the surface migration of HOS molecules is similar to that of the SiH_3 radicals, and the I_{SiH2}/I_{SiH} ratio is localized by the deposition of HOS molecules. Moreover, the results of optical emission spectroscopy show that HOS radical generation is irrelevant to the gas flow velocity.

Keywords: a-Si:H films, SiH_2/SiH bond density ratio, plasma CVD, Raman spectroscopy, microscopic FTIR

DOI: 10.1585/pfr.14.4406144

1. Introduction

Because of the rapid expansion of the Internet of Things (IoTs) technology, power supply for IoT devices has become one of the major concerns limiting their expansion [1]. a-Si:H thin film solar cells have attracted considerable attention as power supplies for IoT devices because of their thin, flexible, and light-weight features, as well as their low production cost compared to other solar cells [1]. However, to ensure a-Si:H thin film solar cells remain highly efficient, it is necessary to suppress light-induced degradation [2–10] by lowering the density of the Si-H_2 bonds in a-Si:H films [6]. Therefore, for reducing Si-H_2 bond density, we developed deposition methods [11–17].

A-Si:H films are extensively deposited via a SiH_4 discharge plasma [2–17], which contains one major deposition species of SiH_3 radicals and two minor deposition species: HOS molecules in the size range below 0.5 nm and clusters in the size range above 0.5 nm [12]. To reduce cluster incorporation, we adopted the multi-hollow discharge plasma chemical vapor deposition (MHDPCVD) method together with a cluster-eliminating filter. According to this method, clusters are transported from the discharge region to the vacuum pump via a fast gas flow [14–17]. In this study, we examined the effect of gas velocity on the SiH_2/SiH bond density ratio of the a-Si:H films using Raman spectroscopy, micro-FTIR (Fourier transform infrared) spectroscopy, and optical emission spectroscopy (OES).

2. Experimental

As shown in Fig. 1, we performed deposition experiments using MHDPCVD with a cluster-eliminating filter [14–17]. We deposited a-Si:H films on a 5 cm × 2.5 cm Si substrate. The substrate was set in the upstream region from the electrodes, and the substrate temperature was set at 170°C. Pure SiH_4 was fed from the bottom of the reactor

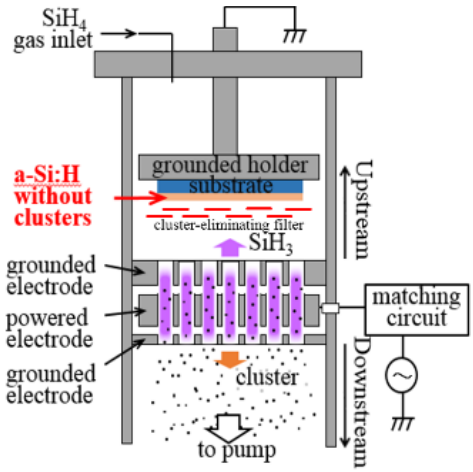

Fig. 1 Multi-hollow discharge plasma reactor with a cluster-eliminating filter.

author's e-mail: l.shi@plasma.ed.kyushu-u.ac.jp

*) This article is based on the presentation at the 2nd Asia-Pacific Conference on Plasma Physics (AAPPS-DPP2018).

at 56 - 147 sccm, and then passed through 89 holes in the electrodes; moreover, the diameter and length of each hole were 5.0 and 10.0 mm, respectively. The total pressure was 0.08 Torr. We applied high-frequency discharge voltage of 110 MHz to the powered electrode with a discharge power of 20 W. Discharges were mainly sustained in the hollows, where radicals and clusters were generated and transported outside the hollows via diffusion or gas viscosity. Figure 2 shows the dependence of the diffusion velocity of particles generated in the discharge on their size. The diffusion velocity v_d is expressed as follows:

$$v_d = \frac{D}{\Lambda}, \quad (1)$$

where D is the diffusion coefficient of the particles and Λ is the characteristic diffusion length. Λ was assumed to be equal to the length of the hollows. For a gas velocity of 1500 cm/s, particles with sizes >0.5 nm were driven to the downstream region, while particles with sizes <0.5 nm were transported toward the substrate set in the upstream region because of their fast diffusion. For a gas velocity of 2646 cm/s, particles with sizes >0.36 nm were driven to the downstream region; however, the size of the HOS radicals ranged between 0.36 and 0.5 nm. Thus, by increasing the SiH_4 gas velocity, we succeeded in suppressing the incorporation of HOS molecules into the films. We set a cluster eliminating filter between the electrodes and the substrate. The cluster transmission probability of the filter was <1%; therefore, a-Si:H films without incorporated clusters were deposited in the upstream region by combining the MHD-PCVD reactor with a cluster-eliminating filter.

We performed Raman spectroscopy using a Raman spectrometer (JASCO NRS-3100) equipped with the second harmonics of CW Nd:YAG laser light (λ = 532 nm) excitation. The exposure time was 100 s, and the integration number of scans was 3. The diameter of the probe laser was 1 μm. We measured seven positions on each sample. The Raman spectrum of the films was in the range of 1800 - 2300 cm^{-1}. It was deconvoluted into two Gaussian profiles with peaks at 2090 and 2000 cm^{-1}, corresponding to Si-H_2 bonds and Si-H bonds in a-Si:H films. Using the intensities of these two peaks, we calculated the SiH_2/SiH bond density ratio I_{SiH2}/I_{SiH}.

Moreover, the ratio I_{SiH2}/I_{SiH} was measured with a microscopic FTIR spectrometer (IRT-7200). The spectral resolution was 4 cm^{-1}, and the integration number of the scans was 64. Using this method, we obtained two-dimensional profiles in a 1.5 mm × 1.5 mm square region from the transmission spectra of the samples. The spatial resolution was 50 μm × 50 μm, and a total of 900 points were measured in 30 rows and 30 columns. The surface morphology of the films was characterized using an atomic force microscope (AFM, Bruker DimensionIcon). The scanned surface area was 1 × 1 μm^2. The AFM images were analyzed using the image processing software Gwyddion.

3. Results and Discussion

Figure 3 shows the gas velocity dependence of I_{SiH2}/I_{SiH}, which was confirmed using the Raman spectroscopy results. The ratio decreased from 0.18 for the gas velocity of 1008 cm/s to 0.1 for the gas velocity of 1500 cm/s, which suggests that the lower incorporation of HOS molecules into the films resulted in lower Si-H_2 bond concentration in the films. For a gas velocity of >1512 cm/s, the ratio decreased slightly to 0.086 at 2646 cm/s, indicating that few HOS molecules are deposited on the films when the gas velocity exceeded 1512 cm/s. Furthermore, such a high gas velocity reduced the gas residence time in the discharge space and suppressed the formation of clusters and HOS molecules. Eventually, such a contribution of clusters and HOS molecules to film formation reduced I_{SiH2}/I_{SiH} at high gas velocity.

Figure 4 shows the spatial distribution of the SiH_2/SiH bond density ratio depending on the gas velocity. The ratio significantly decreases with increase in gas velocity from 1008 to 2646 cm/s. Furthermore, the in-plane uniformity is improved at a higher gas velocity. Figure 5 shows the frequency distribution of the spatial distribution of the

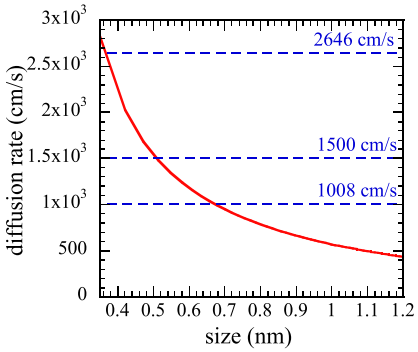

Fig. 2 Dependence of diffusion velocity on the size of the particles generated in the plasma.

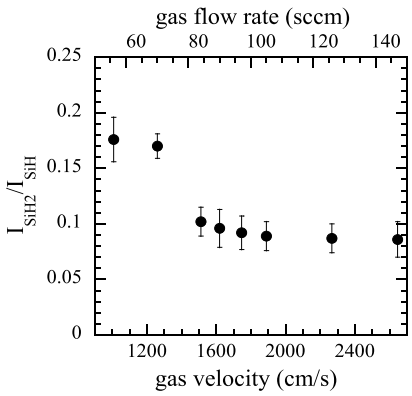

Fig. 3 Gas velocity dependence of I_{SiH2}/I_{SiH} of a-Si:H films.

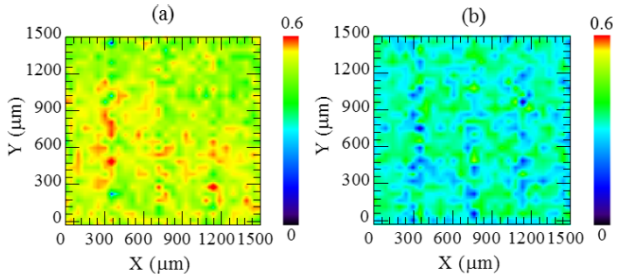

Fig. 4 Spatial distribution of SiH_2/SiH bond density ratio for a gas velocity of (a) 1008 cm/s and (b) 2646 cm/s.

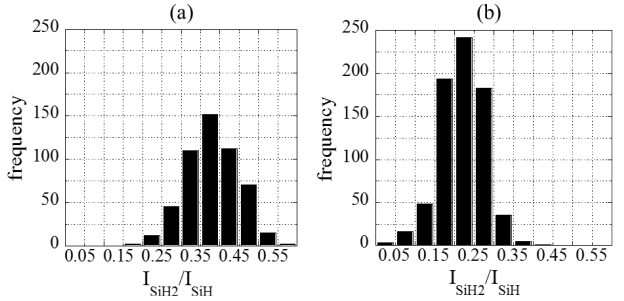

Fig. 5 Frequency distribution of SiH_2/SiH bond density ratio for a gas velocity of (a) 1008 cm/s and (b) 2646 cm/s.

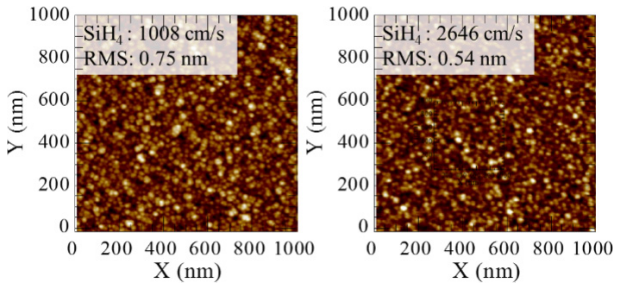

Fig. 6 AFM images of a-Si:H films for a gas velocity of 1008 cm/s and 2646 cm/s (scan size: 1 μm × 1 μm).

SiH_2/SiH bond density ratio at 1008 and 2646 cm/s, obtained from the results shown in Fig. 4. The frequency distribution range decreases with increasing gas velocity. The results suggest that the incorporation of HOS molecules are localized, leading to an in-plane uniformity peak shift and peak broadening in the frequency distribution of the SiH_2/SiH intensity ratio.

As shown in Fig. 6, to examine the effects of the HOS molecules on film growth, we obtained AFM images of a-Si:H films deposited on Si substrates for 1008 and 2646 cm/s. The root-mean-square (RMS) roughness of the films is slightly decreased from 0.75 nm for a gas velocity of 1008 cm/s to 0.56 nm for a gas velocity of 2646 cm/s. This indicates that the deposition of HOS molecules does not have a significant impact on the RMS roughness. Figure 7 shows the height-height correlation function (HHCF) of the AFM images for gas velocities of 1008 and 2646 cm/s. HHCF analysis is a useful method for analyzing surface morphology. The HHCF function H(r) is expressed as follows [18–20]:

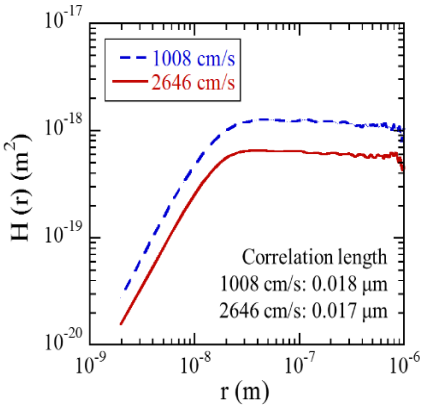

Fig. 7 Height-height correlation function calculated from the AFM images for a gas velocity of (a) 1008 cm/s and (b) 2646 cm/s.

$$H(r) \sim \begin{cases} Cr^{2\alpha} & (r \ll \xi) \\ 2\omega^2 & (r \gg \xi) \end{cases}, \quad (2)$$

where r is the distance between two positions in the AFM image, C is a constant, α is the local roughness exponent, ξ is the correlation length, and ω is the surface roughness. Note that ξ is the length at which the HHCF functions shows an inflection point, and it is considered a measure of the surface diffusion length [21, 22]. The results in Fig. 7 show that the correlation lengths for gas velocity values at 1008 and 2646 cm/s are 0.018 and 0.017 μm, respectively. This means that SiH_3 radicals and HOS molecules have similar surface mobilities; however, according to the present experimental results, the SiH_2/SiH bond ratio of a-Si:H films with HOS molecules is higher, and the contribution of such HOS molecules is reduced at a higher gas velocity.

To obtain information on the gas velocity dependence of HOS generation, we performed OES measurements because Si^* (λ = 288.2 nm, $4s^1P^0$-$3p^21D$) and SiH^* (λ = 414 nm, $A^2\Delta$-$X^2\Pi$) emission intensities tend to be proportional to the SiH_x radical generation rate. Moreover, we analyzed their ratio Si^*/SiH^*, which is correlated with electron temperature [23, 24]. The results are shown in Fig. 8. There is no significant change in the emission intensities of Si^* and SiH^* as well as in the intensity ratio Si^*/SiH^* with increase in gas velocity from 1008 to 2646 cm/s, i.e., electron temperature and radical generation do not change considerable when the gas velocity exceeds 1008 cm/s. Therefore, the generation of HOS molecules in plasma is irrelevant to the gas velocity.

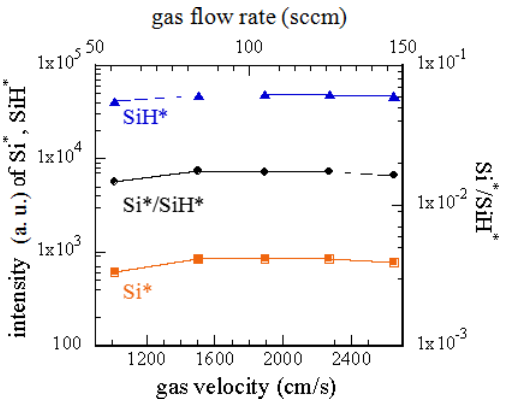

Fig. 8 Gas velocity dependence of emission intensity of Si^* and SiH^* and the intensity ratio Si^*/SiH^*.

Table 1 Deposition of particles for three conditions and relation between precursors and SiH_2/SiH bond density ratio of a-Si:H films.

		SiH_3 radicals	higher-order silane (HOS)	clusters
Conventional method		○	○	○
MHDPCVD method cluster-eliminating filter	v_g (1008 cm/s)	○	○	×
	v_g (2646 cm/s)	○	×	×
SiH_2/SiH bond density ratio of a-Si:H films		low	high	highest

4. Conclusions

In this study, we examined whether the deposition of SiH_3 radicals contributed to the bonding configuration of hydrogenated amorphous silicon (a-Si:H) films. The results are summarized in Table 1. Overall, we deposited a-Si:H films on Si substrates by controlling the gas velocity with a MHDPCVD reactor coupled with a cluster-eliminating filter. We examined the SiH_2/SiH bond density ratio of the a-Si:H films using Raman spectroscopy and microscopic FTIR spectroscopy. We succeeded in suppressing the incorporation of clusters and HOS molecules into the films and obtained an extremely low SiH_2 bond density film by increasing the gas velocity from 1008 to 2646 cm/s. Finally, increasing the SiH_4 gas velocity was confirmed to be effective for suppressing SiH_2 bond formation in a-Si:H films.

Acknowledgments

This work was partly supported by AIST and JSPS KAKENHI Grant Number JP26246036. Both film deposition and Raman spectroscopy were carried out at the Center of Plasma Nano-Interface Engineering (CPNE), Kyushu University. Similarly, microscopic FTIR and AFM measurements were conducted at the Center of Advanced Instrumental Analysis, Kyushu University.

[1] A. Raj and D. Steingart, J. Electrochem. Soc. **165**, B3130 (2018).
[2] D.L. Staebler and C.R. Wronskj, Appl. Phys. Lett. **31**, 292 (1977).
[3] D.L. Staebler and C.R. Wronski, J. Appl. Phys. **51**, 3262 (1980).
[4] M. Konagai, H. Takei, W.Y. Kim and K. Takahashi, Proc. 18th IEEE PVSC, 1372 (1985).
[5] K. Tanaka, J. Non-Cryst. Solids **137-138**, 1 (1991).
[6] T. Nishimoto, M. Takai, H. Miyahara, M. Kondo and A. Matsuda, J. Non-Cryst. Solids **299-302**, 1116 (2002).
[7] S. Nunomura, I. Sakata and M. Kondo, Appl. Phys. Express **6**, 126201 (2013).
[8] S. Nunomura and I. Sakata, AIP Adv. **4**, 097110 (2014).
[9] S. Nunomura, I. Sakata and K. Matsubara, J. Non-Cryst. Solids **436**, 44 (2016).
[10] S. Nunomura, I. Sakata and K. Matsubara, Appl. Phys. Express **10**, 081401 (2017).
[11] K. Koga, N. Kaguchi, K. Bando, M. Shiratani and Y. Watanabe, Rev. Sci. Instrum. **76**, 113501 (2005).
[12] K. Koga, T. Inoue, K. Bando, S. Iwashita, M. Shiratani and Y. Watanabe, Jpn. J. Appl. Phys. **44**, L1430 (2005).
[13] M. Shiratani, K. Koga, N. Kaguchi, K. Bando and Y. Watanabe, Thin Solid Films **506**, 17 (2006).
[14] W.M. Nakamura, H. Matsuzaki, H. Sato, Y. Kawashima, K. Koga and M. Shiratani, Surf. Coat. Technol. **205**, S241 (2010).
[15] S. Toko, Y. Hashimoto, Y. Kanemitu, Y. Torigoe, H. Seo, G. Uchida, K. Kamataki, N. Itagaki, K. Koga and M. Shiratani, J. Phys.: Conf. Ser. **518**, 012008 (2014).
[16] Y. Hashimoto, S. Toko, D. Yamashita, H. Seo, K. Kamataki, N. Itagaki, K. Koga and M. Shiratani, J. Phys.: Conf. Ser. **518**, 012007 (2014).
[17] K. Koga, W.M. Nakamura and M. Shiratani, Proc. 28th ICPIG, 1987 (2007).
[18] Y.-B. Park, S.-W. Rhee and J.-W. Hong, J. Vac. Sci. Technol. B **15**, 1995 (1997).
[19] H.-N. Yang, Y.-P. Zhao, A. Chan, T.-M. U and G.-C. Wang, Phys. Rev. B **56**, 4224 (1997).
[20] Y.-Y. Liu, C.-F. Cheng, S.-Y. Yang, H.-S. Song, G.-X. Wei, C.-S. Xue and Y.-Z. Wang, Thin Solid Films **519**, 5444 (2011).
[21] D. Raoufi, A. Kiasatpour, H.R. Fallah and A.S.H. Rozation, Appl. Surf. Sci. **253**, 9085 (2007).
[22] Z.-J. Liu, N. Jiang, Y.G. Shen and Y.-W. Mai, J. Appl. Phys. **92**, 3559 (2002).
[23] Y. Watanabe, M. Shiratani and K. Koga, *Advanced Plasma Technology*, 227 (John Wiley & Sons, 2008).
[24] S. Toko, Y. Torigoe, K. Keya, T. Kojima, H. Seo, N. Itagaki, K. Koga and M. Shiratani, Surf. Coat. Technol. **326**, 388 (2017).